DOI: https://doi.org/10.24113/ijoscience.v7i12.448

Design and Performance Evaluation of Low-Speed Vertical Axis Wind Turbines with Wind Boosters using CFD Analysis

Sardar Karanjeet Singh
M.Tech Scholar
Truba Institute of Engineering &Information Technology
Bhopal, Madhya Pradesh, India
karanjeetsingh5550@gmail.com

Shravan Vishwakarma
Assistant Professor
Truba Institute of Engineering &Information Technology
Bhopal, Madhya Pradesh, India

Abstract: **The use of wind based energy is quickly expanding over the planet. The goal of this study is to use computational methods of fluid dynamics to develop a novel model of VAWT including Windbooster for various rotor blades like two, three, and four blades in order to enhance effectiveness. CAD modelling approaches of vertical axis wind turbines including and excluding booster are created. Including all vertical axis wind turbine blade designs including and excluding booster, torque, power, and Coefficient of performance are compared.The performance of three blades on the basis of mechanical properties includingi wind amplifier is 29.9% greater than two blades using wind amplifier, and four blades using wind amplifier is 21.5 percent greater than three blades using wind amplifier, according to the findings. Because the mechanical energy created by a four-blade wind booster wasn't as great as it is including three blades, VAWT employing three-blade wind booster seems to be more effective than VAWT with a two- or four-blade wind booster. For improved mechanical durability, VAWT with three-blade wind amplifier is recommended.**

Keywords*:* Wind Turbine, CFD, VAWT, Wind Boosters.

I. Introduction

Wind energy technology is accelerating all over the earth. Resulting in high technical advances, the competence of the sector, and rising worries about greenhouse gas emissions connected to burning of fossil fuels, the usage of wind to produce electricity is fast increasing. Albeit a limited amount of the serviceable wind potential is now employed, despite the vast wind resources. The speed with which wind based energy is adopted is influenced by government and energy industry laws, along with government subsidies.

This source of energy has also been extensively used in European nations. Wind energy is mostly used in Germany, Denmark, and Spain. Denmark aims to generate 40% of its electricity through wind turbines by 2025. The United Kingdom has the most wind energy supplies, which should be expanded to lower wind energy costs. The Global Wind Energy Council (GWEC) just released the Worldwide Wind Energy Report. Document. In 2016, the worldwide economy for wind power developed over than 54 GW. According to GWEC's five-year prediction, roughly 60 GW of additional wind turbines will also be erected by 2017 and a 75 GW yearly marketplace will be established by 2021, bringing overall installed capacity including over 800 GW by the ending of 2021.

Alternative techniques, in addition to wind turbines, are constantly evolving. Turbine blades based drones, for instance, transmit and utilize as much wind energy as possible before returning it via cables. Wind energy can also be harnessed using kites.

II. Literature Review

Natapol Korprasertsak et al. [1] The inquiry and optimal design of wind flow management components for a VAWT termed as the Wind-booster are presented in this study. Wind-booster with a VAWT is designed not only to generate electricity with little ease of access at lower wind speeds, but also to progressively strengthen VAWT implementation at higher speeds of the wind . By this investigation, the proposed methodology can be used to determine the best breeze boosters for various dimensions of wind turbines.

Andreas Wibowo et al. [2] The primary purpose of this investigation is to determine the ideal configuration between both the aide balancing and the cross-stream vertical pivot wind turbine, taking into account a range of variables such as the aide balancing' point of ability and the number of turbine sharp corners and guiding vanes. In comparison to the basic structure excluding the structure of a guide vane, the results indicated that with a specific setup, the aide vane may significantly increase the force generated by the wind turbine by 271.39 percent.

AbdolrahimRezaeiha et al. [3] The effect of drag (s) and quantity of edges (n) on the streamlining implementation of 2, 3, and 4 cutting edge vertically pivot wind turbines (VAWT) of the Darrieus H. kind within the broad scope from 0.09 to 0.36 is effectively subdivided in this study. To estimate the effect of sen on distinctive burdens on the cutting edges, the demonstration of the turbine, and the caster, a huge proportion of organizational limits are examined, including the biggest speed ratio (l), the Reynolds number (Re), the power of the disruption, and the reduced recurrence (K).

PongchalatChaisiriroj et al. [4] This work concentrates on a strategic plan for examining the demonstration of perfect vertical hub wind turbines (VAWTs) in Thailand that are modified to low wind speed circumstances. The results will also reveal wild factors of real-world activity that are not depicted in the programme simulations but have an impact on turbine performance, such as strong particles, unsettled breeze speed, and the surroundings. The findings of the investigation are presented so that they can be used as a manual to perform on the design and development of VAWT.

II. OBJECTIVE

- ❖ The goal of this study is to use CFD analysis to develop a new configuration of VAWT including wind booster for various blades including two, three, and four blades in order to achieve better performance.
- ❖ CAD modelling approaches of vertical axis wind turbine blades including and excluding boosters are being created.
- ❖ Implement CFD simulation on all layouts of vertical axis wind turbine blades, including those with and without boosters.
- ❖ Torque, power, and power coefficient for all vertical axis wind turbine blade designs with and without booster

III. METHODOLOGY

Algorithm used for Computational fluid dynamics analysis

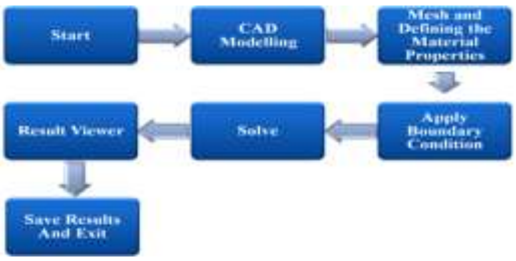

Fig. 1: Algorithm employed for Computational fluid dynamics analysis

Governing Equations

The formula for mass conservation, also known as the continuity equation, can be expressed in terms:

$$\frac{\partial \rho}{\partial t} + \nabla.(\rho\, \vec{v}) = S_m$$

Where Sm denotes the amount of mass incorporated to the continuous phase or whatever other user-defined information. The continuity equation for two dimensional axisymmetric configurations is:

$$\frac{\partial \rho}{\partial t} + \frac{\partial}{\partial x}(\rho v_x) + \frac{\partial}{\partial r}(\rho v_r) + \frac{\rho v_r}{r} = S_m$$

The axial coordinate is x, the radial co - ordinates is r, the axial velocity is v x, and the radial velocity is v r.

Equation is derived of Conservation of Momentum:

In an inertial reference frame, momentum conservation is characterized by

$$\frac{\partial}{\partial t}(\rho\vec{v}) + \nabla.(\rho\vec{v}\vec{v}) = -\nabla p + \nabla.(\bar{\bar{\tau}}) + \rho\vec{g} + \vec{F}$$

Where p= static pressure

$\bar{\bar{\tau}}$ = stress tensor,

$\rho\vec{g}$ = gravitational body force and

$\vec{F}$ = external body forces

The stress tensor $\bar{\bar{\tau}}$ is given by

$$\bar{\bar{\tau}} = \mu\left[(\nabla\vec{v} + \nabla\vec{v}^{\mathrm{T}}) - \frac{2}{3}\nabla.\vec{v}I\right]$$

where μ = molecular viscosity

I = unit tensor,

For 2D axisymmetric geometries, the axial and radial momentum conservation equations are given by

$$\frac{\partial}{\partial x}(\rho v_x) + \frac{1}{r}\frac{\partial}{\partial x}(r\rho v_x v_x) + \frac{1}{r}\frac{\partial}{\partial r}(r\rho v_r v_r) = -\frac{\partial p}{\partial x} + \frac{1}{r}\frac{\partial}{\partial x}\left[r\mu\left(2\frac{\partial v_x}{\partial x} - \frac{2}{3}(\nabla.\vec{v})\right)\right] + \frac{1}{r}\frac{\partial}{\partial r}\left[r\mu\left(\frac{\partial v_x}{\partial r} + \frac{\partial v_r}{\partial x}\right)\right] + F_x$$

And

$$\frac{\partial}{\partial t}(\rho v_r) + \frac{1}{r}\frac{\partial}{\partial x}(r\rho v_x v_r) + \frac{1}{r}\frac{\partial}{\partial r}(r\rho v_r v_r) = -\frac{\partial p}{\partial r} + \frac{1}{r}\frac{\partial}{\partial x}\left[r\mu\left(\frac{\partial v_r}{\partial x} + \frac{\partial v_x}{\partial r}\right)\right] + \frac{1}{r}\frac{\partial}{\partial r}\left[r\mu\left(2\frac{\partial v_r}{\partial r} - \frac{2}{3}(\nabla.\vec{v})\right)\right] - 2\mu\frac{v_r}{r^2} + \frac{2\mu}{3r}(\nabla.\vec{v}) + \rho\frac{v_z^2}{r} + F_r$$

Where

$$\nabla.\vec{v} = \frac{\partial v_x}{\partial x} + \frac{\partial v_r}{\partial r} + \frac{v_r}{r}$$

Where v_x= Axial velocity

v_r= Radial velocity

$\boldsymbol{v_z}$ = swirl velocity

Energy Equation:

The energy equation for the mixture takes the following form:

$$\frac{\partial}{\partial t}\sum_{k=1}^{n}(\alpha_k\rho_k E_k) + \nabla.\sum_{k=1}^{n}\left(\alpha_k\vec{v}_k(\rho_k E_k + p)\right) = \nabla.\left(k_{eff}\nabla T\right) + S_E$$

Where k_{eff} = effective conductivity &S_E = volumetric heat sources

$$E_k = h_k - \frac{p}{\rho k} + \frac{v_k^2}{2}$$

Where

$E_k = h_k$ for an incompressible phase and h_k= sensible enthalpy for phase k

$k{-}\in model$:

The turbulence kinetic energy, k, and its rate of dissipation, $\in$, are obtained from the following transport equations: $\frac{\partial}{\partial t}(\rho k) + \frac{\partial}{\partial x_i}(\rho k v_i) = \frac{\partial}{\partial x_j}\left[\left(\mu + \frac{\mu_t}{\sigma_k}\right)\frac{\partial k}{\partial x_j}\right] + G_k + G_b - \rho \in - Y_M + S_k$ And

$$\frac{\partial}{\partial t}(\rho \in) + \frac{\partial}{\partial x_i}(\rho \in v_i) = \frac{\partial}{\partial x_j}\left[\left(\mu + \frac{\mu_t}{\sigma_\in}\right)\frac{\partial \in}{\partial x_j}\right] + C_{1\in}\frac{\in}{k}(G_k + C_{3\in}G_b) - C_{2\in}\rho\frac{\in^2}{k} + S_\in$$

In these equations, G_k represents the generation of turbulence kinetic energy due to the mean velocity gradients,

G_b = Generation of turbulence kinetic energy due to buoyancy,

Y_M = Fluctuating dilatation in compressible turbulence to the overall dissipation rate,

$C_{1\in}$, $C_{2\in}$, and $C_{3\in}$ are constant. σ_k and $\sigma_\in$ are turbulent Prandtl numbers for k and $\in$,

S_k And $S_\in$ are user-defined source terms

Analysis of two blades excluding a booster using CFD for Vertical Axis Wind Turbine

ANSYS design modular is used to generate a two-dimensional CAD model of a two-blade vertical axis wind turbine for CFD assessment. Figure 4.2 shows a blade consisting of a radius of 97 mm and a height of 250 mm, with a fluid region of 3000 mm x 6000 mm.

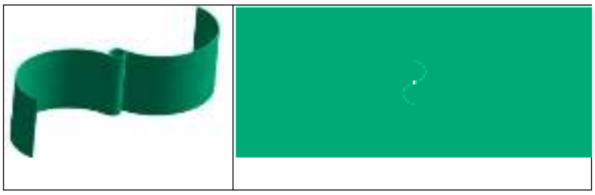

Fig. 2 CAD model of two blades without wind booster for VAWT

Meshing:

The overall number of components on the blade profile is describes as, 1000 are on the blade, 200 here on the hub, and 50 here on end of the blade edge, with a sum of 29702 nodes and 27517 components produced in the ongoing project. Quad8, a rectangular shape including four nodes on every component, is one of the sets of features employed.

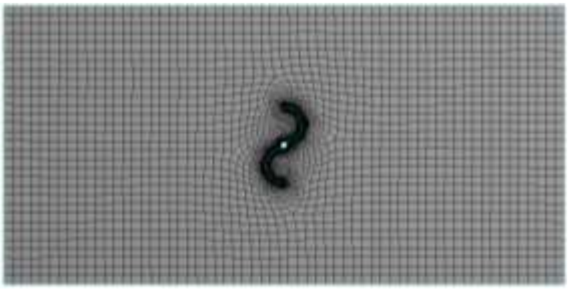

Fig. 3: Meshing of two blades without wind booster for VAWT

Evaluation of two blades including a wind booster using CFD simulation for Vertical axis wind turbine:

ANSYs software modular is used to develop a 2D CAD model of a two-bladed vertical axis wind turbine for CFD software assessment. Including a blade having the radius of 97 mm and also a height of 250 mm, the external and internal diameters of the wind booster are 600 mm and 400 mm, respectively, and the height of the booster is 250 mm, a virtual region for circulation of wind with dimensions of 3000 mm x 6000 mm is generated, as seen in figure 4.

Fig. 4: CAD model of two blades with wind booster for VAWT

Meshing:

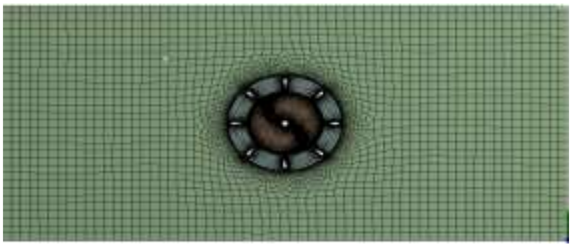

Fig. 5: Meshing of two blades with wind booster for VAWT

The overall number of components on the blade profile is defined as 1000 are on the blade, 200 here on the hub, and 50 here on blade edge side, and the overall number of nodes yielded in this research is 62711, with a complete number of components of 90182. The components employed are rectangular in shape, that have four nodes on every side and are rectangular shaped.

Computational fluid dynamics (CFD) analysis of three blades for VAWT excluding the use of a wind-booster

A virtual region for circulation of wind having the dimensions of 3000 mm x 6000mm was generated with a blade which has the radius of 97 mm and a blade that have height of 250 mm, as seen in figure 6.

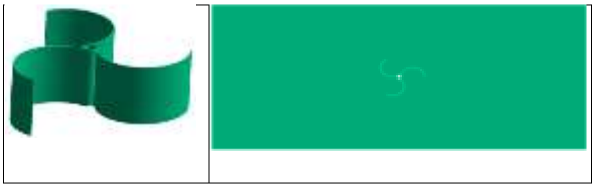

Fig. 6: CAD model of two blades without wind booster for VAWT

Meshing:

The total number of components on the blade profile is 1000 on the blade, 200 here on the hub, and 50 on the blade edge side, and the overall number of nodes obtained in this research is 44049, with a total number of elements of 40797. The components employed are rectangular in shape, which consist of four nodes on every side and are rectangular shaped.

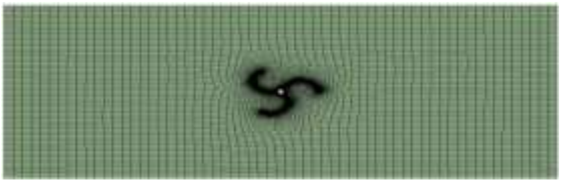

Fig. 7: Meshing of two blades lacking wind booster for VAWT

Assessment of three blades including a wind booster using CFD analysis for VAWT:

As seen in figure 4.8, Comprising a blade with radius of 97 mm and a height of 250 mm, the external and internal diameters of the wind booster are 600 mm and 400 mm, correspondingly, as well as the height of the booster is 250 mm, a virtual area for circulating wind is generated with a dimension of 3000 mm x 6000 mm,

Fig. 8: CAD model of three blades through wind booster for VAWT

Meshing:

The overall number of components on the blade profile is 1000 on the blade, 200 here on the hub, and 50 on the side of the blade edge, with a sum of 68872 nodes and 103995 components created in the ongoing project. The components employed are rectangular shaped, that comprised of four nodes on every side and are rectangular shaped.

Fig. 9: Meshing of three blades with wind booster for VAWT

Assessment of computational fluid dynamics (CFD) of four blades with no need for a wind booster for VAWT:

Figure 10 shows a virtual region for wind circulation generated with a radius of 97 mm and a height of 250 mm, including a dimension of 3000 mm x 6000 mm.

Fig. 10: CAD model of four blades without wind booster for VAWT

Meshing:

The complete number of components on the blade profile is presented as 1000 on the blade, 200 here on hub, and 50 on the edge of the blade edge, with a combined amount of 86827 nodes and 113599 components produced in the current work. The components employed are rectangular, which have four nodes on every side and are rectangular shaped.

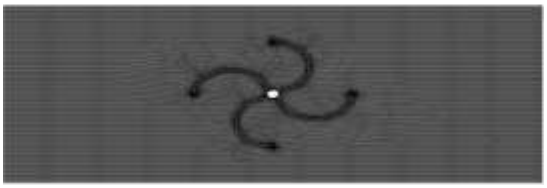

Fig. 11: Meshing of four blades without wind booster for VAWT

Computational fluid dynamics investigation of four blades through wind booster for VAWT:

Fig. 12: CAD model of four blades with wind booster for VAWT

As seen in fig. 13.ith a blade which have the radius of 97 mm and a height of 250 mm, the exterior and interior diameters of the wind booster are 600 mm and 400 mm, including both, and the height of the booster is 250 mm, a virtual region for wind circulation is generated with dimensions of 3000 mm x 6000 mm, .

Meshing:

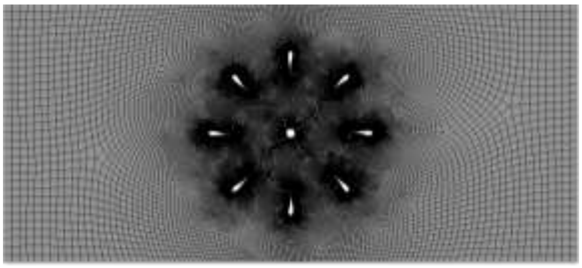

Fig. 13: Meshing of four blades with wind booster for VAWT

The complete number of components on the blade profile is presented as 1000 on the blade, 200 here on hub, and 50 on the side of the blade edge, with a complete number of nodes of 89025 and overall number of components of 130599. The components employed are rectangular in shape, that comprised of four nodes on each side and are rectangular shaped.

Boundary condition

- Generate a virtual fluid region to simulate the circulation of air all over wind turbine blades.
- Employ a highly precise system with a 64 bit system for node coordinate values to estimates the amount more precise.
- Establishment of steady state absolute velocity compositions relying on pressure for CFD assessments

- Choose k-epsilon with enhanced wall treatment procedure turbulence model in the viscous framework.
- Assume the working fluid is air, which has a density of 1.225 kg/m3.6. 6
- Because of the free-stream condition at infinite space, the virtual fluid region limit is fixed as far-field (Far-field circumstances are employed to model a free-stream situation at infinity).
- To study the effectiveness of the VAWT, implement wind speeds ranging from 1 to 8 m/sec.
- At the exhaust boundary limit, the air circulation is maintained at atmospheric levels. Fixed as a wall the blade as well as other far-fields.
- Then choose 2nd order equations for pressure, momentum, and turbulence circulation as governing equations in the option monitoring tab.
- Smooth solver is employed to solve computational fluid dynamics difficulty.

IV. Results

Figure 14 shows the results of a CFD software analysis of two blades excluding booster for Vertical axis wind turbine: the highest velocity at the blade tip was 1.905 m/sec, and the mean speed above the blade was 0.43 m/sec..

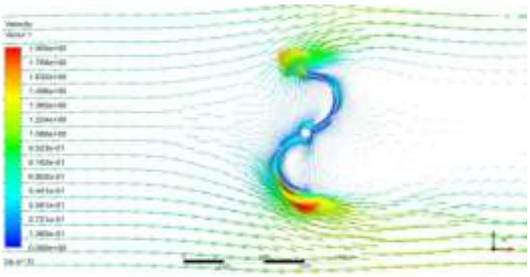

Fig. 14: Wind velocity vector diagram for two blades without wind booster at 1/sec air flow

As seen in fig. 15, the peak value of velocity at the tip of the blade was 3.214 m/sec, with an average velocity of 0.89 m/sec above the blade.

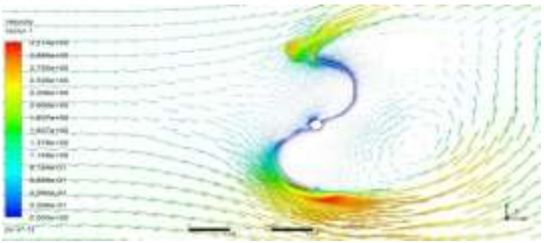

Fig. 15: Wind velocity vector diagram for two blades without wind booster at 2 m/sec air flow

As can be seen in fig. 16, the peak value of the velocity at the tip of the blade was 5.348 m/sec, with an mean velocity of 1.29 m/sec over the blade.

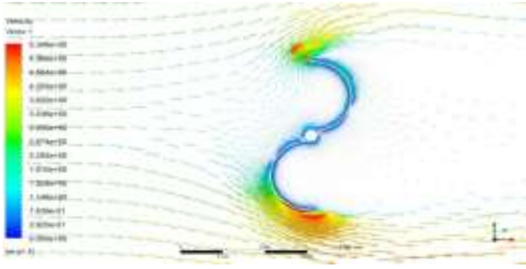

Fig. 16: Wind velocity vector diagram for two blades without wind booster at 3 m/sec air flow

As can be seen in fig. 17, the peak value of velocity at the tip of the blade was 7.083 m/sec, with an mean velocity of 1.71 m/sec over through the blade.

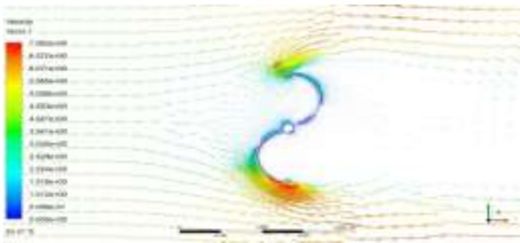

Fig. 17: Wind velocity vector diagram for two blades without wind booster at 4 m/sec air flow

As can be seen in fig. 18, the peak value of velocity at the tip of the blade was 9.053 m/sec, with an mean velocity of 2.15 m/sec above the blade.

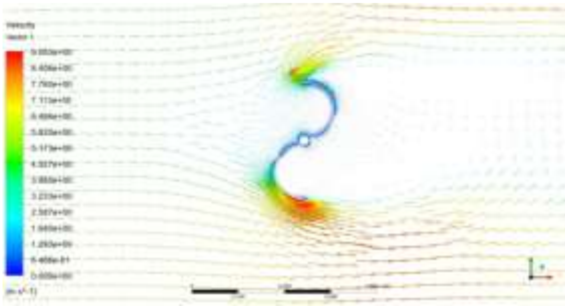

Fig. 18: Wind velocity vector diagram for two blades without wind booster at 5 m/sec air flow

As seen in fig. 19, the peak value of velocity at the tip of the blade was 11.33 m/sec, and the men velocity over the blade was 2.56 m/sec.

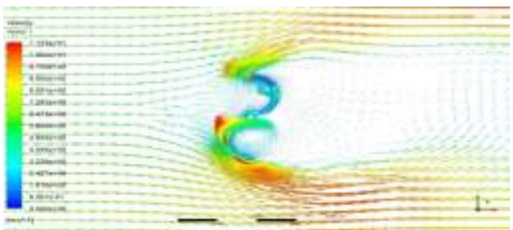

Fig. 19: Wind velocity vector diagram for two blades without wind booster at 6 m/sec air flow

Figure 20 represents the highest velocity at the tip of the blade of 12.91 m/sec and the mean velocity above the blade of 3.01 m/sec.

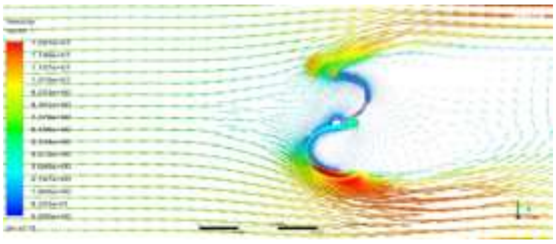

Fig. 20: Wind velocity vector diagram for two blades without wind booster at 7 m/sec air flow

Figure 21 represents the highest velocity at the tip of the blade of 14.57 m/sec and the mean velocity above the blade of 3.45 m/sec.

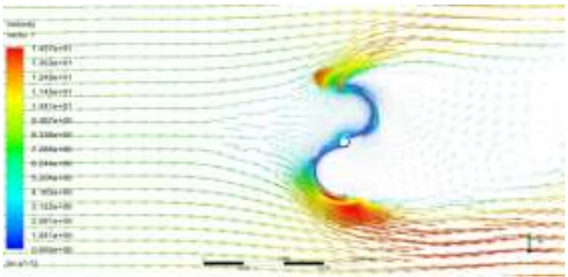

Fig. 21: Wind velocity vector diagram for two blades without wind booster at 8 m/sec air flow

Evaluation of two blades including a booster for Vertical axis wind turbine using computational fluid dynamics:

Figure 22 represents the highest velocity at the tip of the blade of 2.63 m/sec as well as the mean velocity above the blade of 0.65 m/sec.

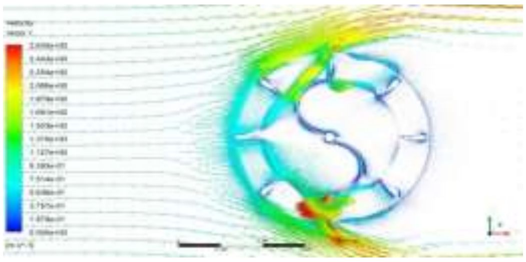

Fig. 22: Wind velocity vector diagram for two blades with wind booster at 1 m/sec air flow

As seen in fig. 23, the peak value of velocity at the tip of the blade was 4.768 m/sec, with an mean velocity of 1.30 m/sec above the blade.

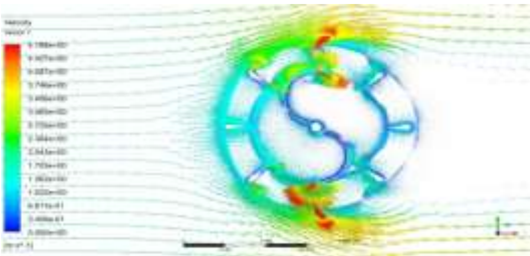

Fig. 23: Wind velocity vector diagram for two blades with wind booster at 2 m/sec air flow

Figure 24 represents the highest velocity at the tip of the blade of 6.451 m/sec as well as the mean velocity over the blade of 1.97 m/sec.

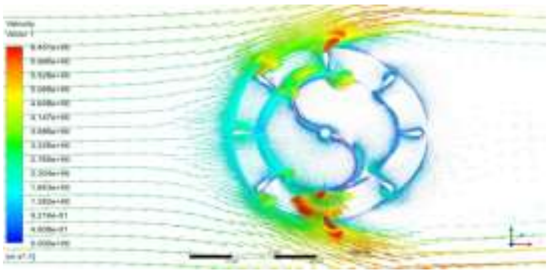

Fig. 24: Wind velocity vector diagram for two blades with wind booster at 3 m/sec air flow

As can be seen in fig. 25, the peak value of velocity at the tip of the blade was 9.522 m/sec, and the mean speed above the blade was 2.62 m/sec.

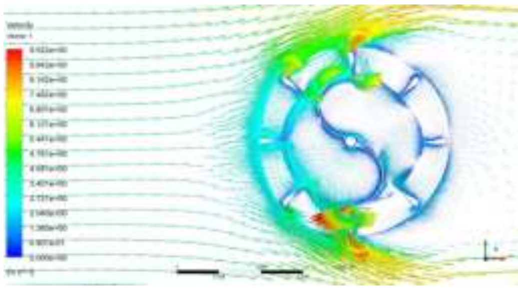

Fig. 25: Wind velocity vector diagram for two blades with wind booster at 4 m/sec air flow

Figure 26 indicates the high velocity at the tip of the blade of 12.19 m/sec as well as the mean velocity above the blade of 3.28 m/sec.

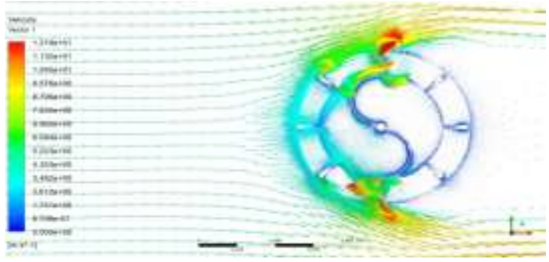

Fig. 26: Wind velocity vector diagram for two blades with wind booster at 5 m/sec air flow

As seen in fig. 27, the peak value of velocity at the tip of the blade was 13.45 m/sec, as well as the mean speed above the blade was 3.91 m/sec.

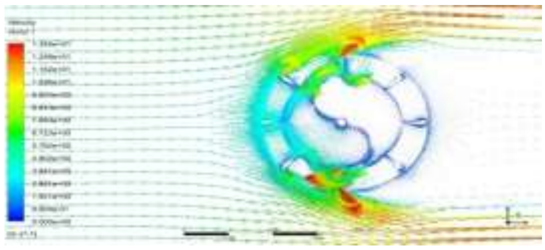

Fig. 27: Wind velocity vector diagram for two blades with wind booster at 6 m/sec air flow

Figure 28 represents the highest velocity at the tip of the blade of 15.73 m/sec as well as the mean velocity above the blade of 4.56 m/sec.

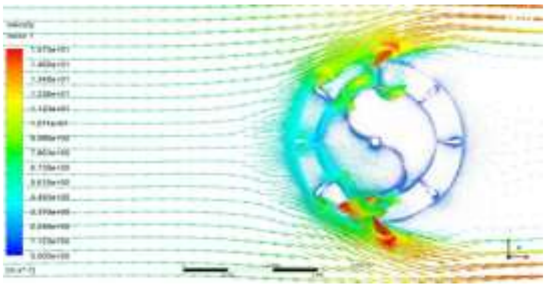

Fig. 28: Wind velocity vector diagram for two blades with wind booster at 7 m/sec air flow

The highest velocity at blade has been captured as 18.15 m/sec at tip of the blade and 5.22 m/sec mean velocity above the blade as represented in fig. 29.

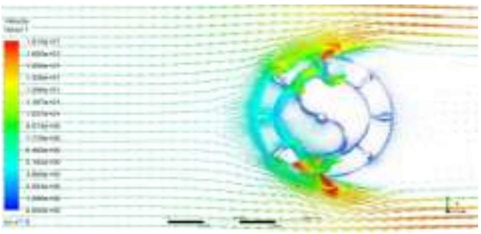

Fig. 29: Wind velocity vector diagram for two blades with wind booster at 8 m/sec air flow

Analysis of three blades excluding a booster using CFD analysis for Vertical axis wind turbine:

Figure 30 represents the highest velocity at the tip of the blade of 1.943 m/sec and the mean velocity above the blade of 0.51 m/sec.

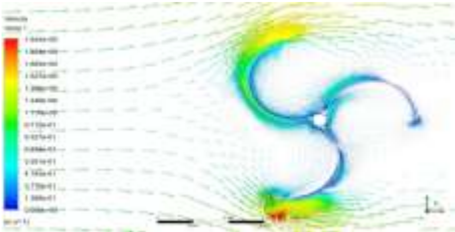

Fig. 30: Wind velocity vector diagram for three blades without wind booster at 1 m/sec air flow

Figure 31 indicates the highest value of velocity at the tip of the blade is 3.379 m/sec and the mean velocity above the blade of 1.06 m/sec.

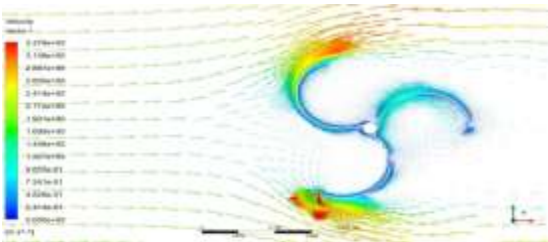

Fig. 31: Wind velocity vector diagram for three blades without wind booster at 2 m/sec air flow

As seen in fig. 32, the peak value of the velocity at the tip of the blade was 6.317 m/sec, as well as the mean velocity about the blade was 1.54 m/sec.

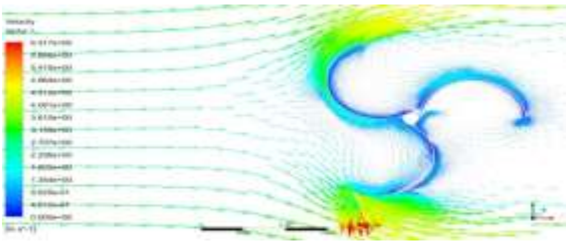

Fig. 32: Wind velocity vector diagram for three blades without wind booster at 3 m/sec air flow

Figure 33 indicates the high velocity at the tip of the blade of 8.211 m/sec as well as the mean velocity above the blade of 2.04 m/sec.

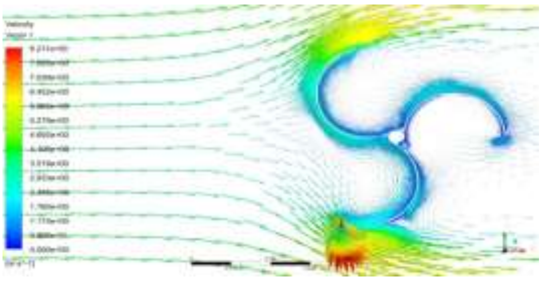

Fig. 33: Wind velocity vector diagram for three blades without wind booster at 4 m/sec air flow

As seen in the fig. 34, the peak valueof velocity at the tip of the blade was 9.774 m/sec, and even the mean velocity above the blade was 2.57 m/sec.

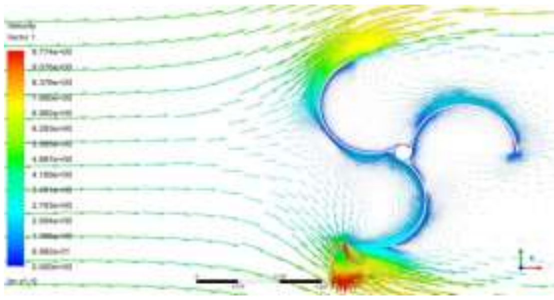

Fig. 34: Wind velocity vector diagram for three blades without wind booster at 5 m/sec air flow

As can be seen in fig. 35, the peak value at the tip of the blade was 11.12 m/sec, and the mean speed over the blade was 3.06 m/sec.

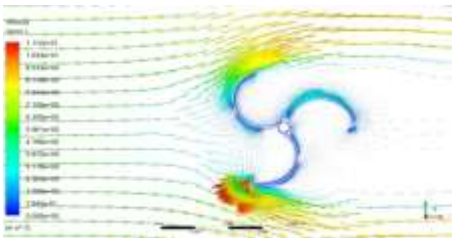

Fig. 35: Wind velocity vector diagram for three blades without wind booster at 6 m/sec air flow

As can be seen in fig. 36, the velocity's peak value at the tip of the blade was 13.14 m/sec, and the mean velocity above the blade was 3.603 m/sec.

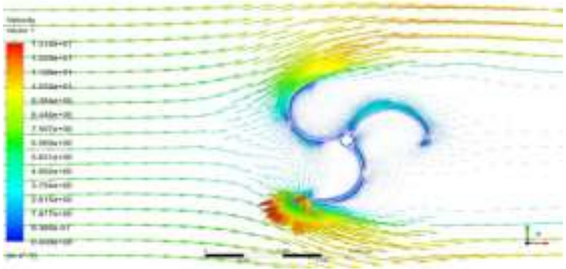

Fig. 36: Wind velocity vector diagram for three blades without wind booster at 7 m/sec air flow

As can be seen in fig. 37, the peak value of velocity at the tip of the blade was 15.12 m/sec, and also the mean velocity above the blade was 4.21 m/sec.

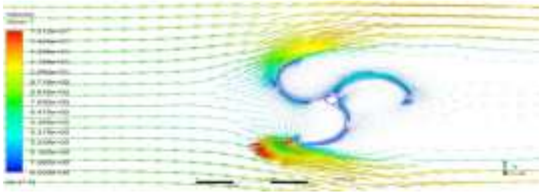

Fig. 37: Wind velocity vector diagram for three blades without wind booster at 8 m/sec air flow

Analysis of three blades including a booster for Vertical axis wind turbine using CFD simulations:

As can be seen in fig.38, the peak value of velocity at the tip of the blade was 2.841 m/sec, with an mean velocity of 0.78 m/sec above the blade.

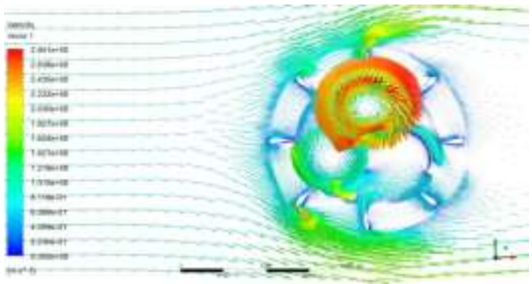

Fig. 38: Wind velocity vector diagram for three blades with wind booster at 1 m/sec air flow

As seen from fig 39, the peak value of velocity at the tip of the blade was 5.720 m/sec, so the mean velocity above the blade was 1.56 m/sec.

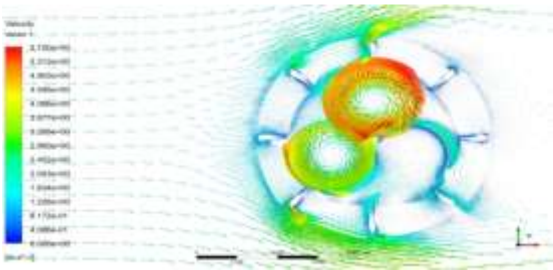

Fig. 39: Wind velocity vector diagram for three blades with wind booster at 2 m/sec air flow

As is shown in the fig. 40, the peak velocity value at the outer edge of blade was 7.250 m/sec, and the mean velocity above the blade was 2.35 m/sec.

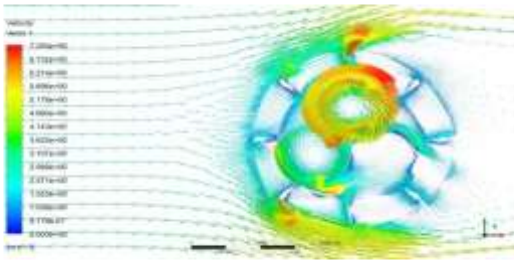

Fig. 40: Wind velocity vector diagram for three blades with wind booster at 3 m/sec air flow

As can be seen in fig. 41, the peak velocity value at the tip of the blade was 8.963 m/sec, and the mean velocity above the blade was 3.13 m/sec.

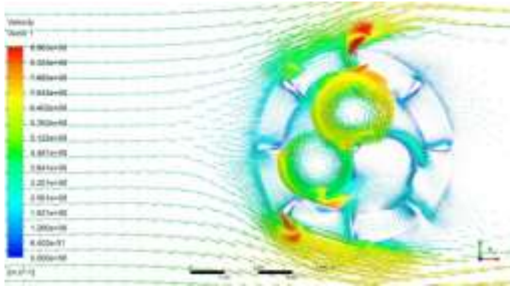

Fig. 41: Wind velocity vector diagram for three blades with wind booster at 4 m/sec air flow

11.10 m/sec is the highest velocity value recorded at blade tip and 3.92 m/sec mean velocity above the blade as depicted in figure 42.

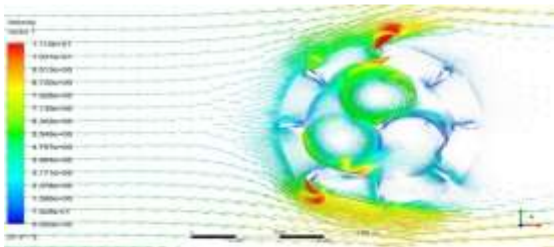

Fig. 42: Wind velocity vector diagram for three blades with wind booster at 5 m/sec air flow

The peakvalue of the velocity at blade has been documented 13.07 m/sec at blade tip and 4.68 m/sec mean velocity over the blade as shown in fig 43.

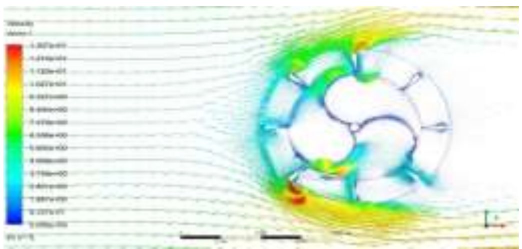

Fig. 43: Wind velocity vector diagram for three blades with wind booster at 6 m/sec air flow

As clearly represented in fig. 44, the highest value of velocity at the tip of the blade was recorded as 15.33 m/sec, with a 5.45 m/sec mean velocity over the blade.

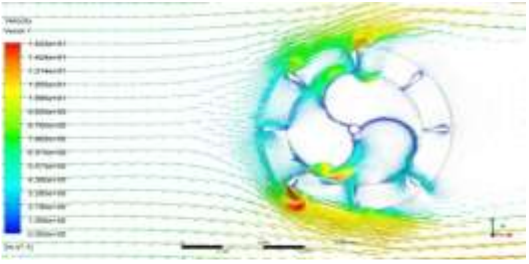

Fig. 44: Wind velocity vector diagram for three blades with wind booster at 7 m/sec air flow

The highest value of velocity at blade has been documented as 17.60 m/sec at blade's tip and 6.23 m/sec mean velocity above the blade as revealed in figure 45.

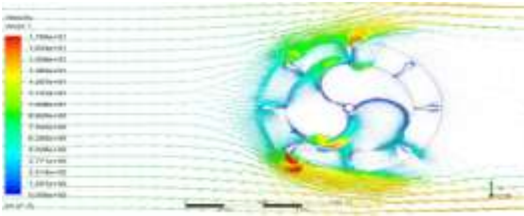

Fig. 45: Wind velocity vector diagram for three blades with wind booster at 8 m/sec air flow

Analysis of four blades excluding a booster using CFD simulation for Vertical axis wind turbine:

As depicted in fig. 46, the peak value of velocity at the tip of the blade was 2.415 m/sec, and the mean velocity above the blade was recorded as 0.654 m/sec.

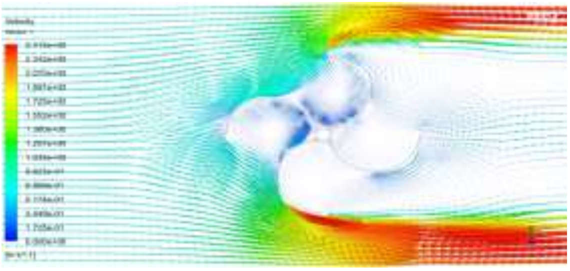

Fig. 46: Wind velocity vector diagram for four blades without wind booster at 1 m/sec air flow

As demonstrated in fig. 47, the highest value of velocity at the tip of the blade was recorded as 6.473 m/sec, with an mean velocity of 1.36 m/sec above the blade.

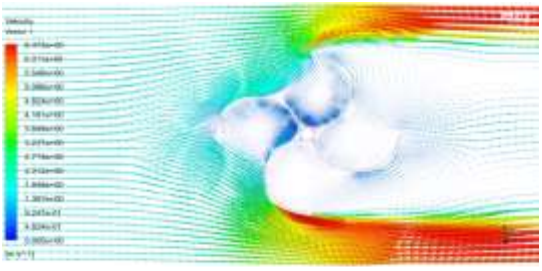

Fig. 47: Wind velocity vector diagram for four blades without wind booster at 2 m/sec air flow

As represented in fig. 48, the peak value velocity at the tip of the blade was 9.716 m/sec, with an mean velocity of 1.97 m/sec over the blade is recorded.

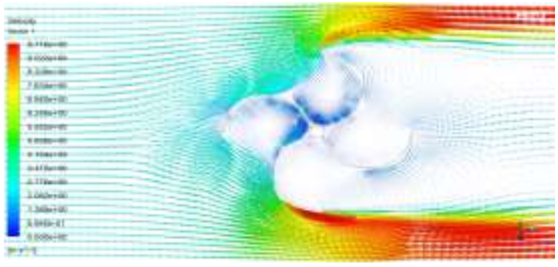

Fig. 48: Wind velocity vector diagram for four blades without wind booster at 3 m/sec air flow

As seen in the fig. 49, the peak value at the tip of the blade was 12.96 m/sec, and the mean velocity over the blade was recorded as 2.62 m/sec.

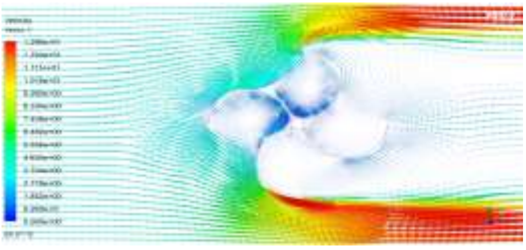

Fig. 49: Wind velocity vector diagram for four blades without wind booster at 4 m/sec air flow

Figure 50 indicates the high velocity at the tip of the blade of 16.22 m/sec and the mean velocity over the blade of 3.29 m/sec.

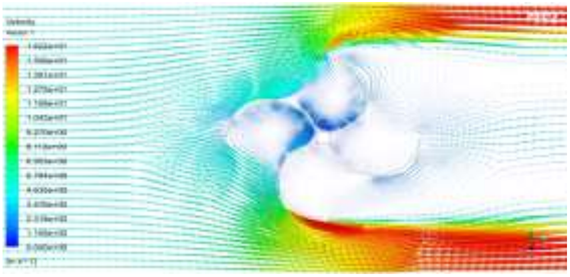

Fig. 50: Wind velocity vector diagram for four blades without wind booster at 5 m/sec air flow

As can be seen in fig. 51, the peak value at the tip of the blade was captured as 19.49 m/sec, and the mean velocity over the blade was 3.92 m/sec.

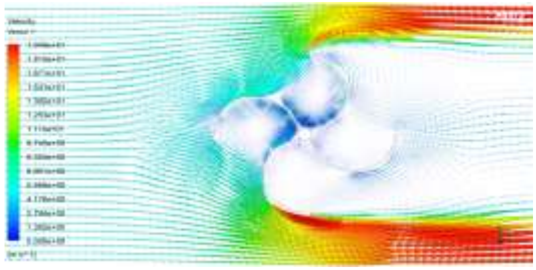

Fig. 51: Wind velocity vector diagram for four blades without wind booster at 6 m/sec air flow

Figure 52 represents the peak value of velocity at the tip of the blade of 20.47 m/sec and the mean velocity over the blade of 4.61 m/sec.

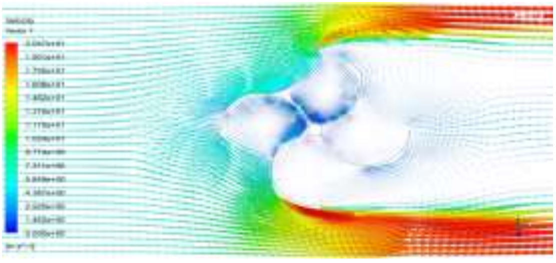

Fig. 52: Wind velocity vector diagram for four blades without wind booster at 7 m/sec air flow

Figure 53 represents the highest velocity at the tip of the blade of 22.12 m/sec and the mean velocity above the blade of 5.28 m/sec.

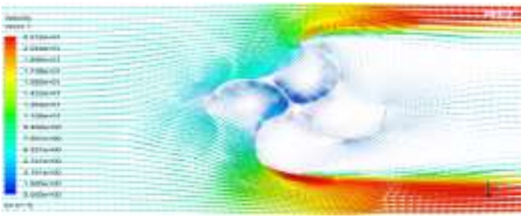

Fig. 53: Wind velocity vector diagram for four blades without wind booster at 8 m/sec air flow

Analysis of four blades including a booster for Vertical axis wind turbine using CFD simulation:

Figure 54 represents the highest velocity at the tip of the blade of 3.658 m/sec and thus the mean velocity above the blade of 0.82 m/sec.

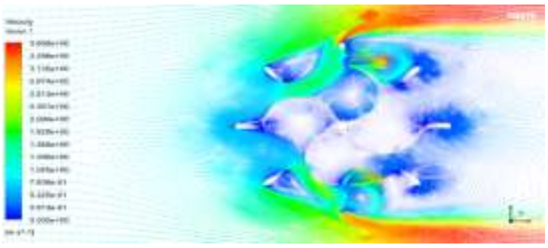

Fig. 54: Wind velocity vector diagram for four blades with wind booster at 1 m/sec air flow

Figure 55 indicates the high velocity at the tip of the blade of 7.509 m/sec and the average velocity so over blade of 1.64 m/sec.

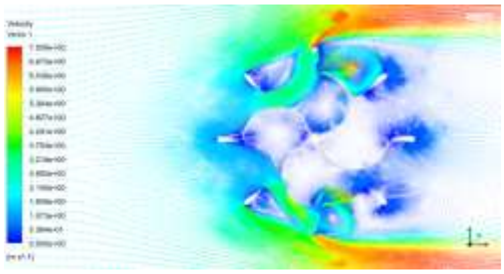

Fig. 55: Wind velocity vector diagram for four blades with wind booster at 2 m/sec air flow

Figure 56 indicates the high velocity at the tip of the blade of 11.62 m/sec and the mean velocity over the blade of 2.47 m/sec.

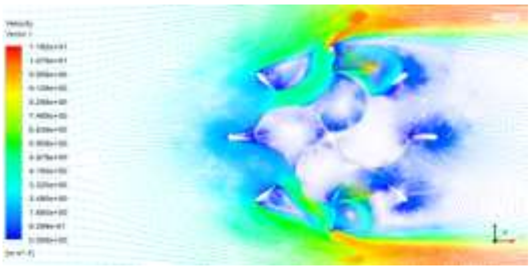

Fig. 56: Wind velocity vector diagram for four blades with wind booster at 3 m/sec air flow

Figure 57 represents the highest velocity at the tip of the blade of 14.87 m/sec as well as the mean velocity over the blade of 3.28 m/sec.

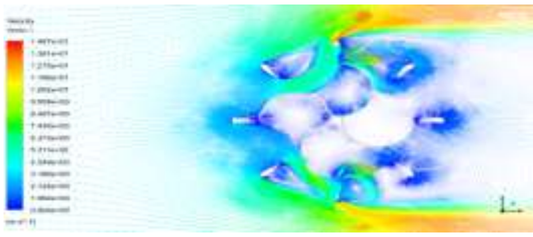

Fig. 57: Wind velocity vector diagram for four blades with wind booster at 4 m/sec air flow

Figure 58 represents the highest velocity at the tip of the blade of 18.08 m/sec and the mean velocity over the blade of 4.12 m/sec.

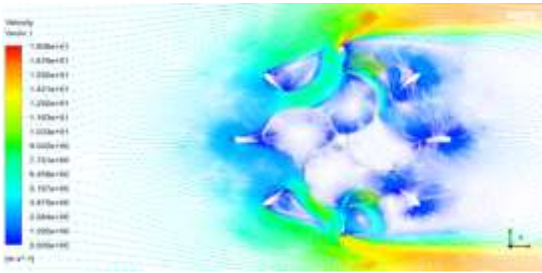

Fig. 58: Wind velocity vector diagram for four blades with wind booster at 5 m/sec air flow

Figure 59 indicates the high velocity at the tip of the blade of 20.72 m/sec and the mean velocity over the blade of 4.91 m/sec.

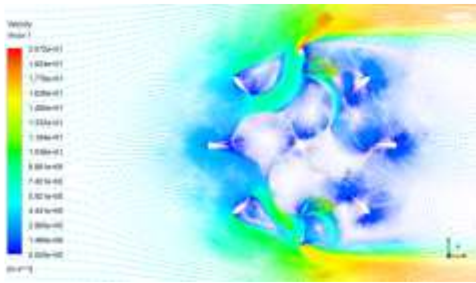

Fig. 59: Wind velocity vector diagram for four blades with wind booster at 6 m/sec air flow

Figure 60 represents the highest value of velocity at the tip of the blade of 22.03 m/sec and the mean velocity over the blade of 5.72 m/sec.

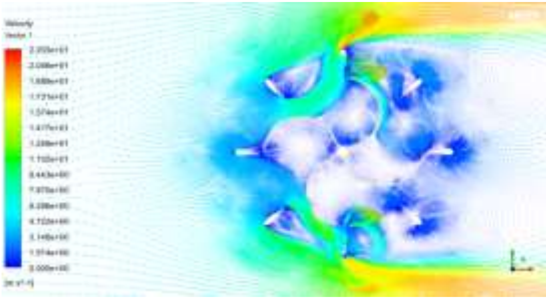

Fig. 60: Wind velocity vector diagram for four blades with wind booster at 7 m/sec air flow

As can be seen in fig. 61, the peak value at the tip of the blade was 23.34 m/sec, and the mean speed above the blade was 6.545 m/sec.

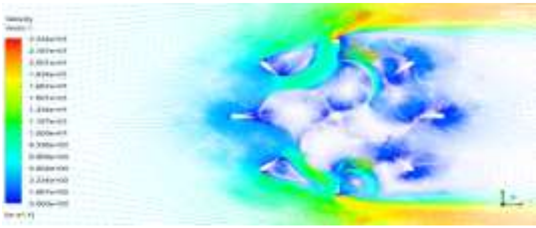

Fig. 61: Wind velocity vector diagram for four blades with wind booster at 8 m/sec air flow

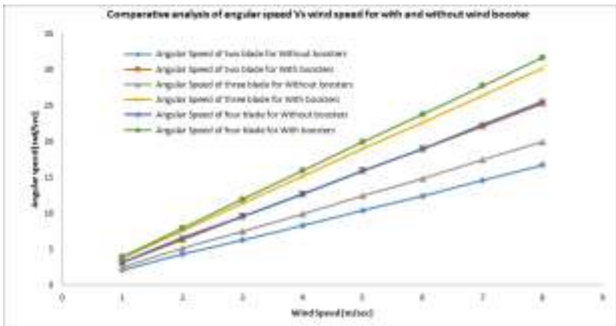

Fig. 62: Comparative analysis of angular speed Vs wind speed for with and without wind booster

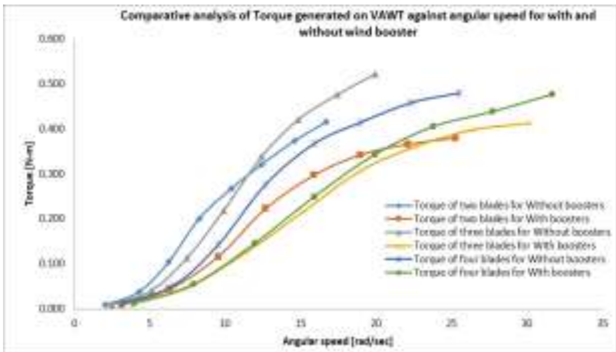

Fig. 63: Comparative analysis of Torque generated on VAWT against angular speed for with and without wind booster

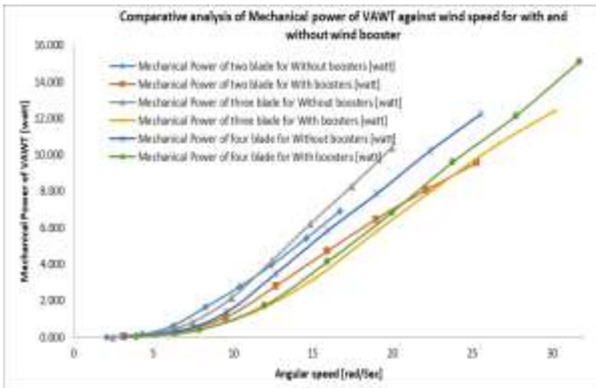

Fig. 64: Comparative analysis of Mechanical power of VAWT against wind speed for with and without wind booster

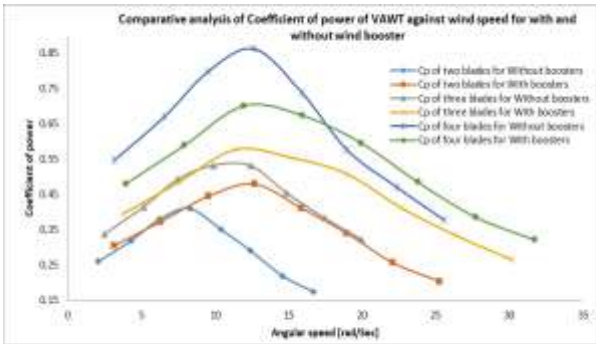

Fig. 65: Comparative analysis of Coefficient of power of VAWT against wind speed for with and without wind booster

V. CONCLUSION

Vertical Axis Fluid Dynamics Numerical methods and Computational Assessment Wind turbines with wind boosters have been tested to improve overall performance of power, torque, and power coefficient. A complete set of six Cad file of VAWTs including and excluding wind booster have indeed been performed to validate. For CFD simulation, a virtual fluid area was generated for air circulation round the blades of wind turbine, and the governing equations were pressure relied on steady state absolute velocity for turbulent model k-epsilon with elevate wall treatment employing second order pressure, momentum, and turbulence circulation. Wind speeds varying from 1 to 8 m/sec were used to test the VAWT's effectiveness while the outlet boundary condition air circulation remained at atmospheric levels. From this assessment, the following are the findings.

❖ After operating analytical and numerical fluid dynamics evaluation of two blades excludingt wind booster for Vertical axis wind turbine at various wind velocity ranging from 1 m/sec to 8 m/sec, the highest value of angular speed 16.7 rad/sec, torque 0.415 N-m, Mechanical power 6.93W, and the maximum COP is 0.41 at 8.28 rad/sec, whereas the highest angular speed 25.26 rad/sec, torque 0.379 N-m, Mechanical power 6.93W, and the maximum value of COP is 0.48 at 12.68 rad/sec. Thus enhancement of angular velocity about 51.25% , torque 9.57%, mechanical power 38.2% and

COP4.9% on comparing vertical axis wind turbine including or excluding wind booster.

- ❖ By operating mathematical and CFD analysis of three blades excluded wind booster for Vertical axis wind turbine at various wind velocity ranging from 1 m/sec to 8 m/sec, the maximum angular speed 19.96 rad/sec, torque 0.522 N-m, Mechanical power 10.42W, and the maximum coefficient of power 0.53 at 9.89 rad/sec were found, while the maximum angular speed 30.19 rad/sec, torque 0.412 N-m, Mechanical power 10.42W, and As a result, angular speed increased by 51.3 percent, torque increased by 26.6 percent, mechanical power increased by 19.38 percent, and the coefficient of power increased by 7.5 percent when compared to when the wind booster Vertical Axis Wind Turbine was not used..
- ❖ And by conducting computational fluid dynamics evaluation of different blades excluding wind booster for Vertical axis wind turbine at various wind wind velocity ranging from 1 m/sec to 8 m/sec, maximum angular angular speed 25.54 rad/sec, torque 0.480 N-m, Mechanical power 12.26W and the maximum coefficient of power 0.86 at 12.67 rad/sec. while for the four blades with wind booster of VAWT at similar wind velocity as not including wind booster the maximum angular speed 31.69 rad/sec, torque 0.477 N-m, Mechanical power 15.12W and the maximum value coefficient of power (COP) 0.702 at 11.97 rad/sec. As a result, angular speed increased by 24.07 percent, torque increased by 0.63 percent, mechanical power increased by 23.3 percent, and coefficient of power increased by 22.5 percent when compared to when the wind booster VAWT was not used.
- ❖ From the foregoing, it can be concluded that using a wind booster improves VAWT performance. Three blades with wind booster have 29.9% more mechanical power than two blades with wind booster and four blades with wind booster. Mechanical power is 57.86 percent higher with wind booster than two blades and 21.5 percent higher with wind booster than three blades. The produced mechanical power is not as high when using four blades with a wind booster as it is when using three blades, and VAWT with three blades is more productive than two and four blade wind boosters. As a result, VAWT with three blades and a wind booster is recommended for improved mechanical strength.

REFERENCE

[1] NatapolKorprasertsak, ThananchaiLeephakpreeda “Analysis and optimal design of wind boosters for Vertical Axis Wind Turbines at low wind speed”, Journal of Wind Engineering and Industrial Aerodynamics, 159 (2016) 9-18.

[2] Andreas Wibowo, DominicusDanardonoDwiPrijaTjahjana, Budi Santoso “Study of turbine and guide vanes integration to enhance the performance of cross flow vertical axis wind turbine”, The 3rd International Conference on Industrial, Mechanical, Electrical, and Chemical Engineering AIP Conf. Proc. 1931, 030043-1–030043-7;.

[3] AbdolrahimRezaeiha, Hamid Montazeri “Towards optimal aerodynamic design of vertical axis wind turbines: Impact of solidity and number of blades”, Energy 165 (2018) 1129-1148.

[4] PongchalatChaisiriroj, NuttapatTinnachote, SaowapakUsajantragul “Experimental Performance Investigation of Optimal Vertical Axis Wind Turbines under Actual Wind Conditions in Thailand”, Energy Procedia, Volume 138, October 2017, Pages 651-656.

[5] ChaianantSranpat, SuchayaUnsakul “CFD-based Performance Analysis on Design Factors of Vertical Axis Wind Turbines at Low Wind Speeds”, Energy Procedia, Volume 138, October 2017, Pages 500-505.

[6] Sahishnu R. Shah, Rakesh Kumar, KaamranRaahemifar “Design, modeling and economic performance of a vertical axis wind turbine”, Energy Reports, 4 (2018) 619-623.

[7] You-Lin Xu, Yi-XinPeng, Sheng Zhan “Optimal blade pitch function and control device for high-solidity straightbladed vertical axis wind turbine”, Applied Energy, 242, (2019) 1613-1625.

[8] Andres Meana-Fernandez, Irene Sol´ıs-Gallego, “Parametrical evaluation of the aerodynamic performance of vertical axis wind turbines for the proposal of optimized designs”, Energy December 26, 2017.